KSCE Journal of Civil Engineering

DOI 10.1007/s12205-019-1055-5

Tunnel Engineering

pISSN 1226-7988, eISSN 1976-3808
www.springer.com/12205

Case Study of Modified H–B Strength Criterion in Discrimination of Surrounding Rock Loose Circle

Rui Wang*, Xianghui Deng, Yaoyao Meng***, Dongyang Yuan****, and Daohong Xia*****

Received May 26, 2018/Revised September 1, 2018/Accepted November 4, 2018/Published Online January 14, 2019

Abstract

Intermediate principal stress is a significant factor when calculate to determine the surrounding rock loose circles. Based on it, this paper is trying to modify the Hoek–Brown strength criterion, and put forwards a theoretical formula of the loose circle radius. The theoretical formula is applied to Shimen Tunnel, and a comparative analysis between theoretical calculations and field test results is conducted. Here are the results as follows: 1) With an increase of intermediate principal stress, the strength of the rock mass increases and the surrounding rock becomes more difficult to break. Consequently, loose circle thickness is gradually reduced and forms a significant negative linear relationship with the Lode parameter. 2) The results indicate that with a decrease of surrounding rock level in a three-lane hard rock tunnel, the radius of the loose circle increases continuously. 3) The results of the field acoustic wave test show that the theoretical calculation values are consistent with the field measurement results. According to above analysis, the deduced formula is feasible.

Keywords: *loose circle, H–B strength criterion, intermediate principal stress, lode parameter, acoustic testing method*

1. Introduction

Since the beginning of the 21st century, underground engineering in China has gone through an unprecedented development. Especially with the development of traffic engineering, the cross-sectional area of the tunnel is getting larger and the geological conditions that need to be traversed becomes more complicated. In an underground chamber excavation, the original stress balance is changed, thereby leading to stress redistribution. An annular rupture zone called surrounding rock loose circle is then formed around the cavity (Dong *et al*., 1994). In this loose circle, rock mass strength is low, fracture is developed and stability is poor. Therefore, the radius of the loose circle must be determined to improve structural design and ensure construction safety.

Current theoretical methods of determining loose circle thickness are involved in elastic medium, plastic mechanics and elastic–plastic mechanics theories. Many scholars have researched on this issue in the past few decades. Fenner (Ren and Zhang, 2001) analysed a yield zone formed around a chamber and suggested a formula for the radius of the yield zone based on the elastic–plastic theory. Meanwhile, the radius of a loose circle was estimated and analysed by Dube according to the elastic–plastic theory (Zhou and Song, 1994). A back analysis method of elastic–plastic displacement based on the same theory was introduced by Li *et al*. (2006). Based on damage theory and double-line damage model, a criterion was proposed by Li *et al*. (2011) to determine the range of a loose circle. The criterion also considered the strain softening characteristic of rock mass. By the utilized of the 'butterfly'-shaped mechanics analysis model and stress wave theory, Sun studied the distribution law of loose circles, then analyzed the influencing factors of loose circle thickness and expounded the supporting mechanism of loose circle (Sun *et al*., 2016) Chen *et al*. (2015), Li *et al*. (2011) and Shen *et al*. (2010) proposed a calculation method, which was based on the Hoek–Brown (H–B) strength criterion for loose circles. Later on, Serranog researched on the issue based on the convergence constraint method and proposed a mathematical expression to determine the radius of a loose circle (Serrano *et al*., 2011).

At present, the H–B strength criterion is widely used in the theoretical analysis of surrounding rock loose circles because it can reflect the intrinsic nonlinear strength criteria of rock, rock mass failure characteristics, the stress of structure interior and surface state (Zhou and Su, 2016). However, the influence of

*Ph.D. Student, School of Civil Engineering and Architecture, Xi'an University of Technology, Xi'an 710048, China & Lecturer, School of Civil & Architecture Engineering, Xi'an Technological University, Xi'an 710021, China (E-mail: wangrui@xatu.edu.cn)
**Professor, School of Civil & Architecture Engineering, Xi'an Technological University, Xi'an 710021, China (Corresponding Author, E-mail: dh_gl@163.com)
***Graduate Student, School of Civil & Architecture Engineering, Xi'an Technological University, Xi'an 710021, China (E-mail: 15291831068@163.com)
****Graduate Student, School of Civil & Architecture Engineering, Xi'an Technological University, Xi'an 710021, China (E-mail: Yuan_Dongyang@163.com)
*****Graduate Student, School of Civil & Architecture Engineering, Xi'an Technological University, Xi'an 710021, China (E-mail: xiadaohong_737@163.com)

intermediate principal stress is often disregarded in calculation of loose chamber areas. Actually, the influence of this stress on rock mass has been confirmed in recent years. When considered intermediate principal stress, the strength of a rock mass can be increased by more than 30% (Xu and Geng, 1985). Later on, the influence of this stress on rock fracture and strength near excavation boundaries was studied using a combined the finite element method with the discrete element method by Cai (2008). The numerical simulation results indicated the generation of parallel fractures and microcracks, and the formation were attributed to material heterogeneity, relatively high intermediate principal stress (σ_2) and zero-to-low minimum principal stress (σ_3). High intermediate principal stress confines rock damage so that microcracks and fractures could be developed only in the direction parallel to σ_1 and σ_2. This stress also slightly influenced the peak strength of the rock near the excavation boundary. Melkoumian *et al.* (2009) validated an explicit solution for both comprehensive and simplified versions of a new 3D H–B yield criterion. At the same time, the solution could be combined with numerical stress modelling codes. Bezalel and John (2010) conducted true triaxial compression tests, in which the specimens were prepared from two siltstone core sections: one above and one below the Chelungpu Fault in Taiwan. For different constant σ_2 and σ_3 magnitudes, the maximum principal stress (σ_1) was raised until reach the post-failure stage and develop a through-going fault. Despite the differences between the properties of the two cores, peak σ_1 increased in all tests when σ_2 was set at higher levels than σ_3; this behaviour contradicted Mohr–Coulomb condition predictions. A true triaxial compressive experiment was performed considering minimum and intermediate principal stresses by Sriapai *et al.* (2013) and he confirmed the effect of intermediate principal stress. Results indicated that modified Lade and 3D H–B criteria overestimated the strength at all levels of σ_3. Coulomb and H–B criteria could not describe salt strengths beyond the condition where $\sigma_2 = \sigma_3$ because they could not incorporate the effect of σ_2. Simulations were conducted using five new artificial neural networks to demonstrate and investigate the behaviour of rock materials under polyaxial loading by Rennie (2014). The effect of intermediate principal stress on intact rock strength was investigated and compared with laboratory results from the literature. Stress state was used as the objective parameter in the model predictions of the artificial neural networks to compare the differences in laboratory testing conditions. In addition, simulations of the artificial neural networks showed that all of the examined rock types were affected by intermediate principal stress. The influences of intermediate principal stress and surrounding rock thickness on the plastic zone of a deep circular tunnel were analysed by Yu *et al.* (2012, 2013).

In summary, intermediate principal stress considerably influences loose circles, therefore it must be considered in calculations. On the basis of the H–B strength criterion, the calculated formula of a loose circle is derived when considering intermediate principle stress and Lode parameters. The calculated radius of a loose circle is compared with actual test results. Meanwhile, the relation between loose circle thickness and Lode parameters are analyzed in this work.

2. Theoretical Analysis of Loose Circle Considering Intermediate Principal Stress

2.1 H–B Strength Criterion and Theoretical Analysis of Loose Circle

The H–B criterion is an empirical failure criterion that establishes the strength of rock/rock masses in terms of major and minor principal stresses (Hua, 2017), it can be shown in Eq. (1):

$$\sigma_1 = \sigma_3 + \sigma_c \left(m_b \frac{\sigma_3}{\sigma_c} + s \right)^{\alpha} \tag{1}$$

$$\begin{cases} m_b = m_i \exp\left(\dfrac{GSI - 100}{28 - 14D} \right) \\ s = \exp\left(\dfrac{GSI - 100}{9 - 3D} \right) \\ \alpha = \dfrac{1}{2} + \dfrac{1}{6}\left[\exp\left(-\dfrac{GSI}{15} \right) - \exp\left(-\dfrac{20}{3} \right) \right] \end{cases} \tag{2}$$

where σ_1 is the major principal stress (MPa); σ_3 is the minor principal stress (MPa); σ_c is the uniaxial compressive strength of the rock (MPa); m_b is an empirical parameter whose value is 0.001–25.0; m_i reflects the hardness degree of the rock and can be obtained by a uniaxial test; S reflects the degree of rock fragmentation and has a value of 0–1; α is related to *GSI*, which is the index of geological strength, as determined by the lithology, structure and discontinuity of the rock mass, and has a value of 0–100; and D is the rock disturbance parameter, whose value is 0–1.0.

Equation (1) is expressed in polar coordinates as follows:

$$\sigma_\theta = \sigma_r + \sigma_c \left(m_b \frac{\sigma_r}{\sigma_c} + s \right)^{\alpha} \tag{3}$$

where σ_θ is the tangential stress and σ_r is the radial stress (MPa).

The radii of excavation, plastic zone and loose circle are r_0, R_0 and R, respectively. The elastoplastic analysis of the tunnel is considered an axisymmetrical problem, and the equilibrium differential equation without physical force is as follow:

$$\frac{d\sigma_r}{dr} + \frac{\sigma_r - \sigma_\theta}{r} = 0 \tag{4}$$

which obtains the following:

$$\sigma_r = \frac{\sigma_c}{m_b}\left[\left(m_b \frac{P_i}{\sigma_c} + s \right)^{1-a} + m_b (1-a) \ln\left(\frac{r}{r_0} \right) \right]^{\frac{1}{1-a}} - \frac{\sigma_c}{m_b} s \tag{5}$$

where P_i is the support resistance.

By substituting Eq. (5) into Eq. (3), then:

$$\sigma_\theta = \frac{\sigma_c}{m_b}\left[m_b(1-a)\ln\left(\frac{r}{r_0}\right)+(m_b\frac{P_i}{\sigma_c}+s)^{(1-a)}\right]^{\frac{1}{1-a}}-\frac{\sigma_c}{m_b}s + \sigma_c\left[m_b(1-a)\ln\left(\frac{r}{r_0}\right)+(m_b\frac{P_i}{\sigma_c}+s)^{(1-a)}\right]^{(\frac{a}{1-a})} \quad (6)$$

According to the definition of broken zone, the tangential stress on the loose zone boundary is initial stress. That is:

$$\sigma_\theta = p_0 \quad (7)$$

where P_0 is the initial stress.

The radius of the loose zone (R) can be obtained using Eqs. (6) and (7).

Equation (6) shows that the radius of the loose zone is related to span r_0, the basic physical and mechanical parameters of the rock mass m_b, GSI, σ_c, construction method D, support parameter P_i and initial stress state P_0.

2.2 Theoretical Analysis of Loose Circle Considering Intermediate Principal Stress

Singh *et al.* (1998) stated that the H–B strength criterion disregarded the effect of intermediate principal stress in its calculation and thus could not accurately reflect the stress–strain characteristics of a rock mass. Therefore, they proposed an H–B strength criterion that considered the effect of intermediate principal stress. The minor principal stress was replaced with the average value between the intermediate and minor principal stresses. The new equation was as follows:

$$\sigma_1 = \sigma_3 + \sigma_c\left[\frac{m_b(\sigma_2+\sigma_3)}{2\sigma_c}+s\right]^a \quad (8)$$

where σ_2 was the intermediate principal stress.

Traditional plastic theory indicates that stress tensor does not affect the yield and Lode parameter or Lode angle is the characteristic parameter of deviatoric stress. Therefore, the plasticity problem can be evaluated by theoretical calculation using the Lode parameter, which can be expressed for considering intermediate principal stress as Eq. (9):

$$\mu_\sigma = \frac{2\sigma_2-\sigma_1-\sigma_3}{\sigma_1-\sigma_3}. \quad (9)$$

The intermediate principal stress can be expressed as follows:

$$\sigma_2 = \frac{\sigma_1(1+\mu_\sigma)+\sigma_3(1-\mu_\sigma)}{2}. \quad (10)$$

By substituting Eq. (10) into Eq. (8), then:

$$\sigma_1 = \sigma_3 + \sigma_c\left[m_b\frac{\sigma_1(1+\mu_\sigma)+\sigma_3(3-\mu_\sigma)}{4\sigma_c}+s\right]^\alpha. \quad (11)$$

When Eq. (11) is transferred into polar coordinates, thus:

$$\sigma_\theta = \sigma_r + \sigma_c\left[m_b\frac{\sigma_\theta(1+\mu_\sigma)+\sigma_r(3-\mu_\sigma)}{4\sigma_c}+s\right]^\alpha \quad (12)$$

which is combined with Eq. (4) to yield the following:

$$\left[\frac{(\sigma_\theta-p_i)r_0}{r\sigma_c}\right]^{\frac{1}{\alpha}} = s+\frac{m_b\sigma_\theta}{\sigma_c}+\frac{m_b(3-\mu_\sigma)(p_i-\sigma_\theta)r_0}{4\sigma_c r}. \quad (13)$$

According to the definition of the loose circle, tangential stress on the loose boundary is equal to initial stress. Thus, when $\sigma_\theta = P_0$, r is the loose circle radius (R) obtained using the Newton iteration method.

Equation (13) shows that the radius of the loose zone is related to span r_0, the basic physical and mechanical parameters of the rock mass m_b, GSI, σ_c, construction method D, support parameter P_i, initial stress state P_0, intermediate principal stress and Lode parameter.

3. Engineering Application

3.1 Brief Description of Project

Shimen Tunnel, which lies between Baoji and Hanzhong, is a separate section of a one-way three-lane tunnel. The tunnel starts at Qingqiaoyi Town and ends at the Maping Temple in Liuba County of Hanzhong City. The left line length of the tunnel is 8,262 m (ZK183+528 to ZK191+790), and the right line length is 8,226 m (YK183+572 to YK191+798).

3.1.1 Geological Conditions

The tunnel is on the south side of the Qinling Mountains. The tectonic units belong to the western part of the fold belt in the South Qinling Mountains. The area does not have evident folds and active fault zones. The face is stable and does not show a falling phenomenon during excavation. The surrounding rock is substantially strong and mainly appears as a block with no noticeable cracks. The surrounding rock is predominantly gneiss that mainly comprises feldspar and quartz with grain structure.

3.1.2 Design Parameters and Construction Method

The clearance width and height are 16.50 and 5.50 m, respectively. The internal curved arch wall is designed as a single span with an inner radius of 7.50 m. Meanwhile, the inner radius of the invert is 21.88 m, and the maximum excavation width is 18 m. The design parameters of the tunnel section and the support parameters of the surrounding rock are shown in Table 1.

Bench method is mainly used during the construction of Shimen Tunnel. During the construction, the design section of tunnel is divided into two parts which are called upper bench and lower bench respectively. By adopted this method, the upper bench is excavated for around 15–30 m firstly, and then excavated the lower bench for the same distance.

3.2 Calculation of Loose Circle Thickness

Existing research indicates that the fault fracture zone in the tunnel can reduce the stability of the surrounding rock (Wang *et al.*, 2017). Therefore, typical sections without fault fracture zones should be selected and calculated in the levels III, IV and

Table 1. Support Parameters of Shimen Tunnel

Level	Initial support						Secondary lining
	C25 concrete (cm)	Bolt (cm)			Steel mesh (cm)	Steel frame (cm)	C30 concrete (cm)
		Location	Length	Space			
III	15	Arch	300	Φ22@120×120	Φ8@25×25	–	45
IV	24	Arch Sidewall	350	Φ22@100×100	Φ8@20×20	I18@100	50
V	26	Arch Sidewall	400	Φ22@100×100	Φ8@20×20	I20b@75	55

Table 2. Support Resistance and Initial Stress

Level	Location	Length (m)	Bulk density (kN/m^3)	Lateral pressure coefficient	Surrounding rock pressure (kPa)	Percentage (%)	Support resistance (kPa)	Geostress (kPa)
III	Arch	357	27	0.10	63.18	20	12.64	9639
	Sidewall				6.32		1.26	7886
IV	Arch	400	26.5	0.15	126.36	40	50.54	10800
	Sidewall				18.95		7.58	7820
V	Arch	172	26.2	0.3	252.72	30	75.82	4644
	Sidewall				75.82		22.75	4118

V surrounding rocks. The support resistance of the surrounding rock (P_i) can be calculated according to the rules for the design of highway tunnels (JTG/T D70-2010), as shown in Table 2. Only self-weight is considered in calculating initial stress, and tectonic stress is disregarded. The calculation results are shown in Table 2.

The parameters m_i, GSI, D are determined based on the surrounding rock integrity, fracture development degree, blasting disturbance and rock strength of the surrounding rock sections. And the parameters m_b, S, α are determined by Eq. (2). The relevant parameters' value is shown in Table 3.

Substitute parameters into Eq. (6), then the value of loose circle thickness can be obtained without considering intermediate principal stress, as shown in Table 4.

The Lode parameter is defined as −1.0, −0.8, −0.6, −0.4, −0.2, 0, 0.2, 0.4, 0.6, 0.8 and 1.0 in Eq. (13). The loose circle thickness calculated by the modified H–B criterion when considers intermediate principal stress can be obtained, as shown in Table 5.

Table 5 shows that as the Lode parameter increases, the loose circle thickness gradually decreases and a negative value is obtained. A regression analysis is conducted between Lode and D, and fitting curves are drawn. The regression equation and correlation coefficients are shown in Table 6, and the fitting curves are obtained in Figs. 1–6.

Intermediate principal stress considerably influences the surrounding rock loose circle. Meanwhile, the Lode parameter is closely related to the loose circle radius. The analysis is as follows:

1) A comparison of the original and modified H–B criteria

Table 3. Geological Parameters of Surrounding Rocks

level	m_i	GSI	D	σ_c (MPa)	m_b	s	α
III	23	42	0.7	94.18	0.950	0.00022	0.510
IV	23	37	0.8	79.33	0.541	0.00007	0.514
V	23	30	0.9	63.18	0.244	0.00001	0.522

Table 4. Loose Circle Calculations based on H–B Criterion

Level	Loose circle thickness (m)	
	Arch	Sidewall
III	1.69	1.34
IV	3.20	2.98
V	3.95	3.74

Table 5. Loose Circle Calculations considering Intermediate Principal Stress in H–B

Lode parameter (μ_σ)	Loose circle thickness (m)					
	III		IV		V	
	Arch	Sidewall	Arch	Sidewall	Arch	Sidewall
−1.0	0.82	0.69	1.79	1.37	2.24	2.10
−0.8	0.45	0.32	1.45	1.02	1.84	1.79
−0.6	0.09	−0.04	1.12	0.67	1.63	1.48
−0.4	−0.26	−0.41	0.80	0.33	1.23	1.15
−0.2	−0.62	−0.77	0.47	0	0.93	0.77
0	−0.96	−1.12	0.15	−0.34	0.64	0.46
0.2	−1.31	−1.47	−0.16	−0.67	0.35	0.15
0.4	−1.65	−1.82	−0.47	−0.99	0.02	−0.12
0.6	−1.98	−2.17	−0.79	−1.31	−0.29	−0.45
0.8	−2.31	−2.50	−1.08	−1.62	−0.57	−0.71
1.0	−2.64	−2.83	−1.37	−1.92	−0.84	−1.04

Table 6. Regression Analysis of Lode Parameters and Loose Circle Thickness

level	Location	Fitting function	Correlation coefficient	Lode value (D=0)
III	Arch	$D = -1.7282\mu_\sigma - 0.9427$	0.9997	−0.54548
	Sidewall	$D = -1.7632\mu_\sigma - 1.1018$	0.9997	−0.62489
IV	Arch	$D = -1.5827\mu_\sigma + 0.1736$	0.9996	0.10969
	Sidewall	$D = -1.6482\mu_\sigma - 0.3145$	0.9995	−0.19081
V	Arch	$D = -1.5364\mu_\sigma + 0.6527$	0.9988	0.42482
	Sidewall	$D = -1.575\mu_\sigma + 0.5073$	0.9990	0.32210

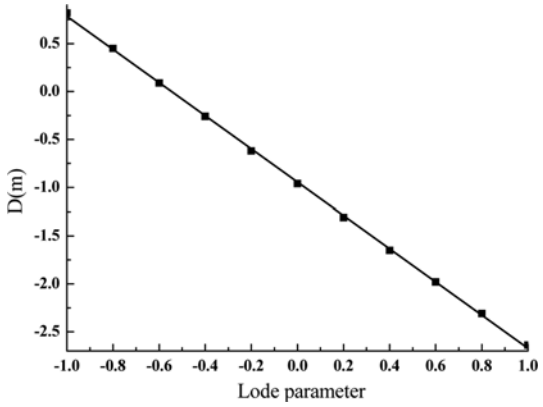

Fig. 1. Level III Arch-fitting Curve

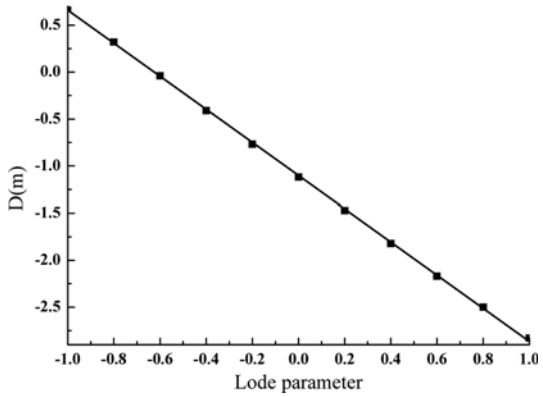

Fig. 2. Level III Sidewall-fitting Curve

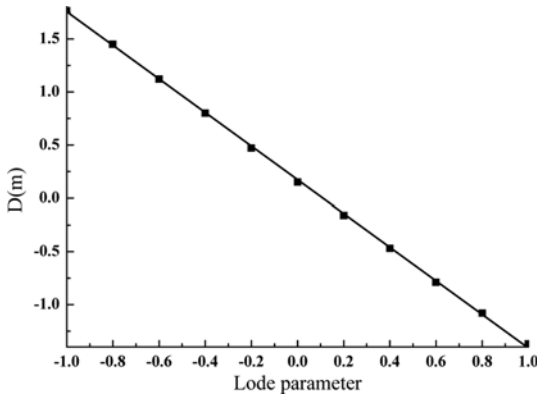

Fig. 3. Level IV Arch-fitting Curve

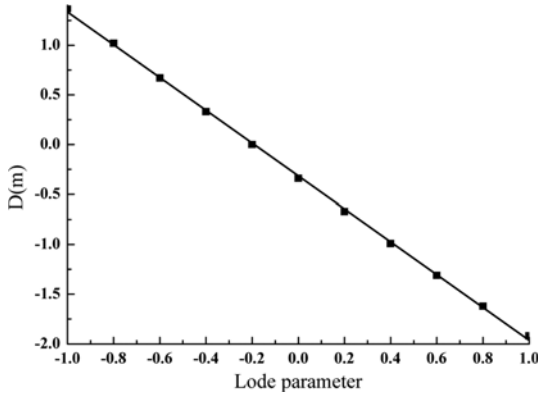

Fig. 4. Level IV Sidewall-fitting Curve

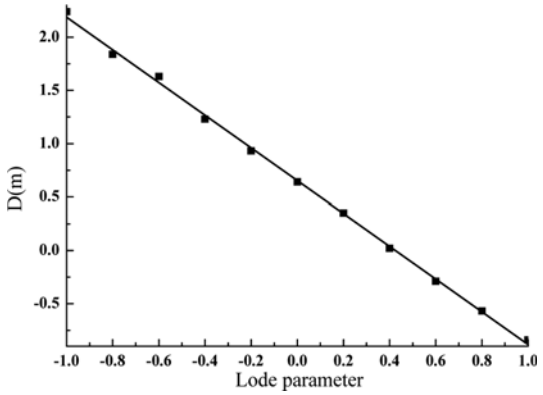

Fig. 5. Level V Arch-fitting Curve

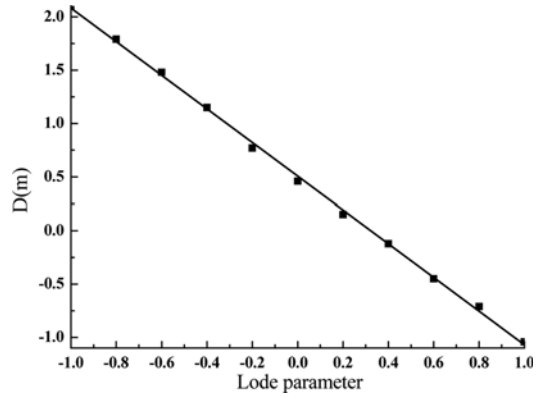

Fig. 6. Level V Sidewall-fitting Curve

indicates that the radius of the loose circle is smaller when intermediate principal stress is considered. Main reason is that the strength of the rock mass increases after considering intermediate principal stress. Consequently, the disturbance on the rock mass is weakened.

2) The radius decreases as the Lode parameter increases. A negative value also appears, which means that with increasing intermediate principal stress, rock strength increases and the surrounding rock becomes difficult to break in a state of stress. Therefore, the loose circle is smaller than not considered, even sometimes does not form.

3) The poorer quality of the surrounding rock, the larger radius of the surrounding rock loose circle can obtain. In levels III, IV and V, when the arch calculation value is zero, the Lode parameters are set as −0.54548, 0.10969 and 0.42482, respectively. In terms of the sidewall, they are −0.62489, −0.19081 and 0.32210, respectively. Therefore, it can be concluded that the poorer the level of the surrounding rock, the larger the value of Lode parameters when the calculation value of loose circle is zero. While the Lode parameters have a proportional relationship with the intermediate principal stress. Although the surrounding rock level is poor, the quality of

the surrounding rock can be improved and the scope of the loose zone can be small when the intermediate principal stress of the rock mass is large.

4) The loose circle thickness of the arch is slightly larger than the value of side wall from Table 5. This is because of the influences of the initial geostress and support force. Over all, the loose circle of surrounding rock is relatively evenly distributed on the cross section.

3.3 Acoustic Method for Testing Loose Circle

3.3.1 Test Scheme

The surrounding rock loose circle can be determined by acoustic techniques because the longitudinal and transversal wave velocities are related to the physical and mechanical characteristics of materials (Frederic and Geraldine, 2007). The single-hole acoustic test method is used in the field test. Four sections, namely, the YK186+025, YK186+110, ZK185+831, ZK185+447 section of levels III are laid out. Four sections, namely, the YK183+590, YK183+610, ZK183+647, ZK184+665 section of levels IV are laid out. Four sections, namely, the YK184+825, YK191+690, ZK183+580, ZK183+550 section of levels V are laid out. Four test holes are laid at each test section considering the surrounding rock condition, section area, data reliability, test operability and test cost of the test section. Two test holes are three meters above the tunnel bottom and they are at the left and right walls of tunnel respectively. The remainder two holes are at the left and right spandrel of tunnel respectively, and the angle between the holes and tunnel centre are 60°. The hole diameter is 40 mm and the depth is 4.0 m. The test holes are perpendicular to the excavation surface. The hole location is shown in Fig. 7, and a schematic of the single-hole acoustic test method is provided in Fig. 8.

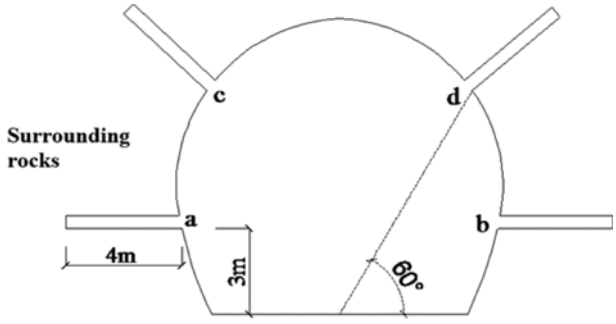

Fig. 7. Hole Layout

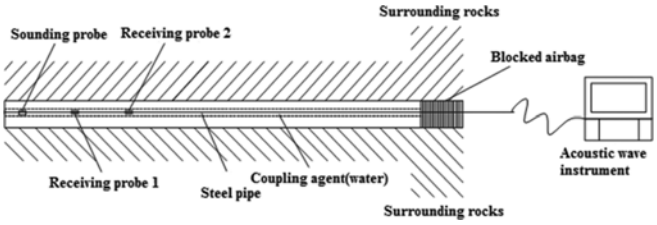

Fig. 8. Test Schematic

Field test is divided into five steps, which are as follows: 1) drilling; 2) cleaning; 3) moving the probe into the measuring hole; 4) closing the hole and coupling; 5) moving the rod and starting the test. Each rod measures 0.5 m, and the test is deemed completed when all rods are consumed.

3.3.2 Criteria for Acoustic Wave Method

According to the wave theory in elastic-plastic media, the velocity of the stress wave is as follows:

$$v_p = \sqrt{\frac{E(1-\mu)}{\rho(1+\mu)(1-2\mu)}} \tag{14}$$

where v_p is the acoustic wave velocity of the surrounding rock; E is the elastic modulus of the surrounding rock; ρ is the surrounding rock density; and u is the poisson's ratio of the surrounding rock.

It can be concluded from Eq. (14) that the acoustic wave velocity of the rock mass is related to the physical and mechanical indexes (v_p, E, ρ and u) of the surrounding rock. In the surrounding rock, if the development of cracks has a large degree and the fracture degree is high, the acoustic wave velocity will be small. Actually, the loose zone is essentially a relaxation fracture zone. Therefore, the velocity of the rock mass in the loose zone is far less than that of the undisturbed surrounding rock. Above all, the position of the loose circle can be determined according to the mutation range of the acoustic wave velocity in the surrounding rock.

At present, there are different views about how to determine the loose circle thickness tested by acoustic wave method. The main discrimination criteria are summarized as follows. 1) While considering economic factor, the point where the acoustic wave of the rock begins to increase substantially, is considered as the judgement basis (Wang *et al*., 2011; Cao *et al*., 2014); 2) While ensuring the safety of construction is given priority, the point where this substantial increase ends, is considered as the judgement basis (Zhang *et al*., 2014; Zhang *et al*., 2016); 3) However some scholars think taking the median point between methods I and II as the judgement basis (Huang *et al*., 2016; Dai *et al*., 2014; Wu *et al*., 2015) is more reasonable. Although the above methods make sense to some extent, the basis in each criterion is insufficient for persuading the latter. Therefore, finding a more objective and accurate method is essential to analyze the variation of acoustic wave velocity in surrounding rock.

The loose of surrounding rock can be determined by the rock mass integrity. Elasticity modulus is an important measure that determines the integrity or failure of brittle materials, and it is proportional to the square of longitudinal wave velocity, as shown in Eq. (14).

The integrity of rock and rock mass can be quantified through longitudinal wave velocity. The integrity coefficients of broken rock (R_v) and loose circle (L_v) are introduced. R_v is the square of ratios between the longitudinal wave after destruction and the longitudinal wave of the complete state, as shown in Eq. (15):

(a) (b) (c)

Fig. 9. Uniaxial Compression and Wave Velocity Tests: (a) Rock Samples, (b) Uniaxial Compression Test, (c) Wave Velocity Test

$$R_V = \left(\frac{v_{pr}}{v_{wr}} \right)^2 \tag{15}$$

where R_v is the integrity coefficient of the broken rock, v_{pr} is the longitudinal wave velocity of the broken rock (km/s) and v_{wr} is the longitudinal wave velocity of the intact rock (km/s).

L_v is the square of the ratios between the longitudinal wave in the position of the broken rock loose circle and the longitudinal wave velocity of the undisturbed rock mass, as shown in Eq. (16):

$$L_v = \left(\frac{v_{pt}}{v_{yt}} \right)^2 \tag{16}$$

where L_v is the integrity coefficient of the loose circle, v_{pt} is the longitudinal wave velocity of the rock mass in the loose zone (km/s) and v_{yt} is the longitudinal wave velocity of the initial rock mass (km/s).

The loose circle is essentially a relaxation fracture zone. Therefore, the integrity coefficient of the loose circle of the surrounding rock can be considered equal to that of the fractured rock of the surrounding rock mass as follows:

$$R_v \approx L_v \tag{17}$$

When Eq. (17) is integrated into Eq. (16), the longitudinal wave velocity of the broken rock (v_{pt}) can be obtained as follows:

$$v_{pt} = v_{yt} \cdot \sqrt{R_v} \tag{18}$$

The longitudinal wave velocity of the rock mass along different radial depths of the tunnel can be obtained through a field test, and the hole depth–wave velocity curve is plotted. With an increase in hole depth, the wave velocity also increases. When the probe penetrates the original rock area, the wave velocity tends to stabilize. At this moment, the longitudinal wave velocity of the original rock mass (v_{yt}) can be obtained. Meanwhile, the longitudinal wave velocity of the fractured rock mass (v_{pt}) is obtained according to Eq. (18). The position where the longitudinal wave velocity value in the curve is equal to v_{pt} is the position of the loose circle. The method proposed uses the degree of surrounding rock's fragmentation to determine the location of loose circle, which has an adequate theoretical basis. So this method is more subjective and accurate than the previous three methods.

3.3.3 Integrity Coefficient (R_v) Test of Fractured Rock

To reflect the integrity coefficient of rock among different surrounding rock levels, levels III, IV and V rock samples are collected on the spot by field sampling and subjected to indoor processing. The samples have a diameter of 50 mm and a height of 100 mm, which are in accordance with the standard test methods for engineering rock mass, and each block comprises 10 sections. Rocks are naturally uneven materials. Thus, the rocks are given similar velocities, structures and occurrences to prevent large dispersion of test data and the occurrence of similar selection of structure, as shown in Fig. 9.

The longitudinal wave velocity (v_{pr}) of the broken rock and the longitudinal wave velocity (v_{wr}) of the intact rock are measured by laboratory testing respectively. Thus, the integrity coefficients (R_v) of the fractured rock can be obtained. The results of v_{pr}, v_{wr} and R_v are shown in Table 7.

The average value of the integrity coefficients of the 10 specimens is considered as the value of broken rock integrity. The R_v values of III, IV and V are 0.53, 0.45 and 0.39, respectively.

3.3.4 Field Test of Loose Circle

The longitudinal wave velocity of the rock mass at different

Table 7. Integrity Coefficient of Fractured Rock

No.	III			IV			V		
	v_{wr} (km/s)	v_{pr} (km/s)	R_v	v_{wr} (km/s)	v_{pr} (km/s)	R_v	v_{wr} (km/s)	v_{pr} (km/s)	R_v
1	6.20	4.61	0.55	6.121	3.756	0.38	5.214	3.458	0.44
2	6.38	4.64	0.53	6.125	3.895	0.40	5.124	3.215	0.39
3	6.23	4.54	0.53	5.869	3.998	0.46	5.231	3.006	0.33
4	6.44	4.48	0.48	5.986	4.112	0.47	5.141	3.121	0.37
5	6.26	4.51	0.52	6.121	4.121	0.45	4.965	3.102	0.39
6	6.27	4.76	0.58	5.768	4.451	0.60	4.786	3.345	0.49
7	6.46	5.07	0.62	5.879	4.135	0.49	5.339	3.214	0.36
8	6.44	4.44	0.48	6.002	4.106	0.47	5.487	3.115	0.32
9	6.27	4.54	0.52	6.254	3.847	0.38	4.999	3.211	0.41
10	6.27	4.51	0.52	5.956	3.958	0.44	5.213	3.451	0.44

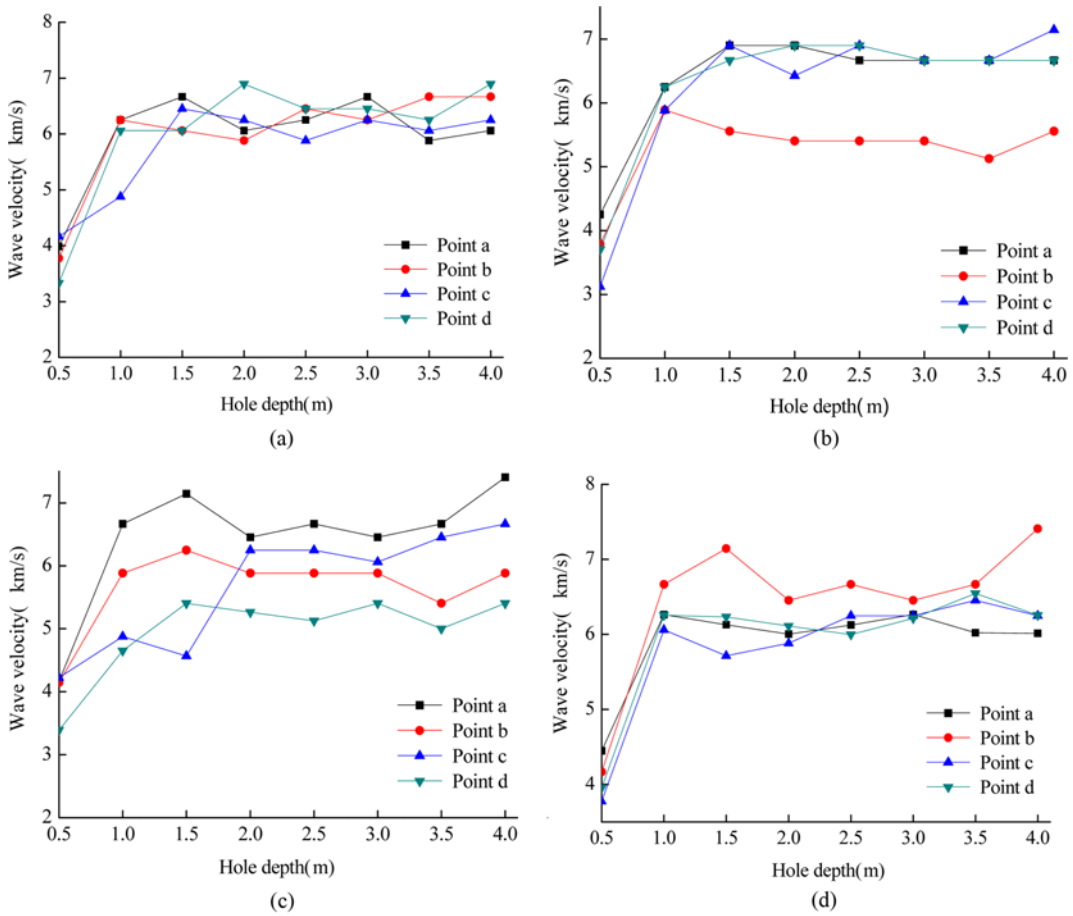

Fig. 10. Hole Depth–wave Velocity Curve of III: (a) YK186+025 Section, (b) YK186+110 Section, (c) ZK185+831 Section, (d) ZK185+447 Section

depths of each monitoring point is measured in each monitoring section, and the depth–wave velocity curves of each section are plotted, as shown in Figs. 10, 11 and 12.

In Figs. 10, 11 and 12, the longitudinal wave velocity of the rock increases with hole depth and gradually stabilizes. The integrity of rock mass also increases with hole depth, whereas the disturbance of the surrounding rock excavation decreases. The deepest part can be regarded as the original rock mass, whose longitudinal wave velocity (v_{yt}) can be obtained. L_v and v_{pt} are computed according to Eqs. (17) and (18), as shown in Table 8. After v_{pt} is calculated, the corresponding vertical coordinate detected in Figs. 10, 11 and 12 is the depth of loose circle, as shown in Table 8.

Based on Table 8, the loose circle thicknesses of III, IV and V are 0.50–0.67, 0.81–1.20 and 1.53–2.07 m in sidewall, respectively. Meanwhile, the arch thicknesses of III, IV and V are 0.60–0.82, 1.09–1.51 and 1.57–2.10 m, respectively. From the results, the arch thicknesses are larger than the sidewall. In addition, the results show that the thickness of the loose circle increases correspondingly when the level of the surrounding rock and the strength of the rock mass are reduced. Overall, the surrounding rock loose circle is evenly distributed, and the vault is slightly larger than the arch waist.

3.4 Comparative Analysis between Theoretical Results and Field Tests

According to the determining parameters, the loose circle thickness is firstly calculated by using the original and modified H–B criteria. We compared the measured data of the loose circle thickness with the theoretical value, and the results are shown as Table 9.

In Table 9, the calculated values of loose circle thickness are larger than the measured values when intermediate principal stress is disregarded. When this stress is considered, the values of loose circle thickness become close to the field test results, which indicates that intermediate principal stress is very important and critically affects loose circle thickness. Since there is no accurate measured value of the intermediate principal stress σ_2, σ_2 is taken the minimum value which means $\sigma_2 = \sigma_3$ in the theoretical calculation from a safety perspective. In the actual engineering, the intermediate principal stress is greater than the minimum principal stress. We concluded that the loose circle thickness decreases as the intermediate principal stress increases. So the theoretical calculation result is slightly larger than the measured result.

The theoretical calculation and measured results indicate that the loose circle thickness ranges of III, IV and V are 0.50–0.82,

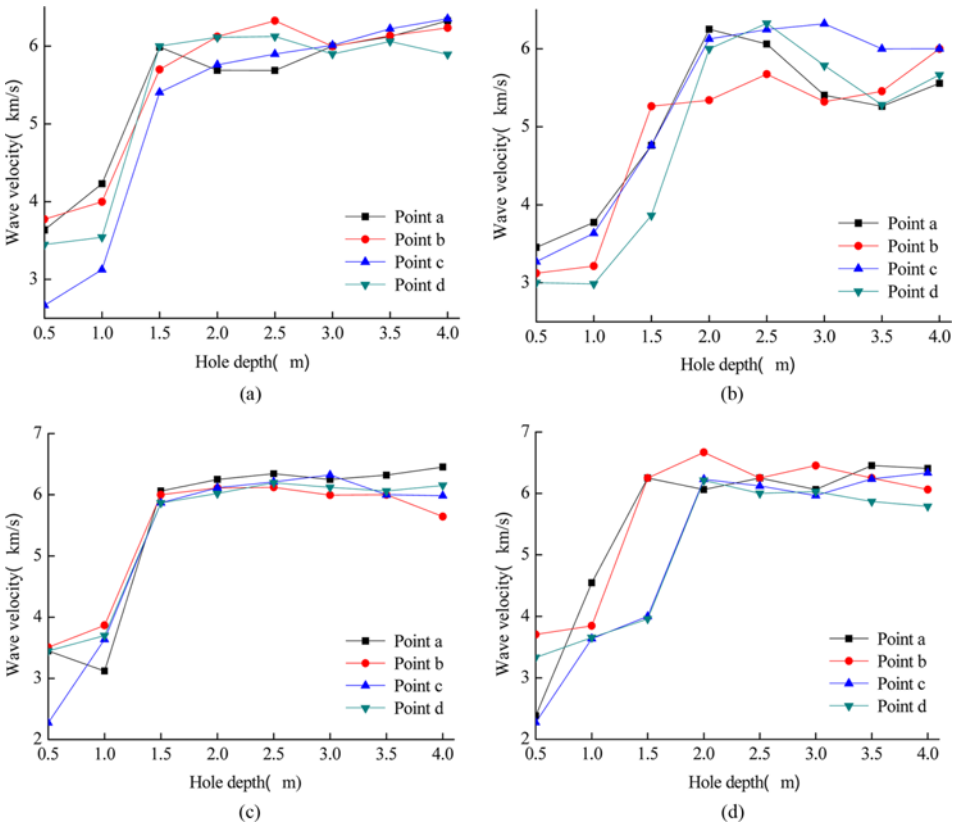

Fig. 11. Hole Depth–wave Velocity Curve of IV: (a) YK183+590 Section, (b) YK183+610 Section, (c) ZK183+647 Section, (d) ZK184+665 Section

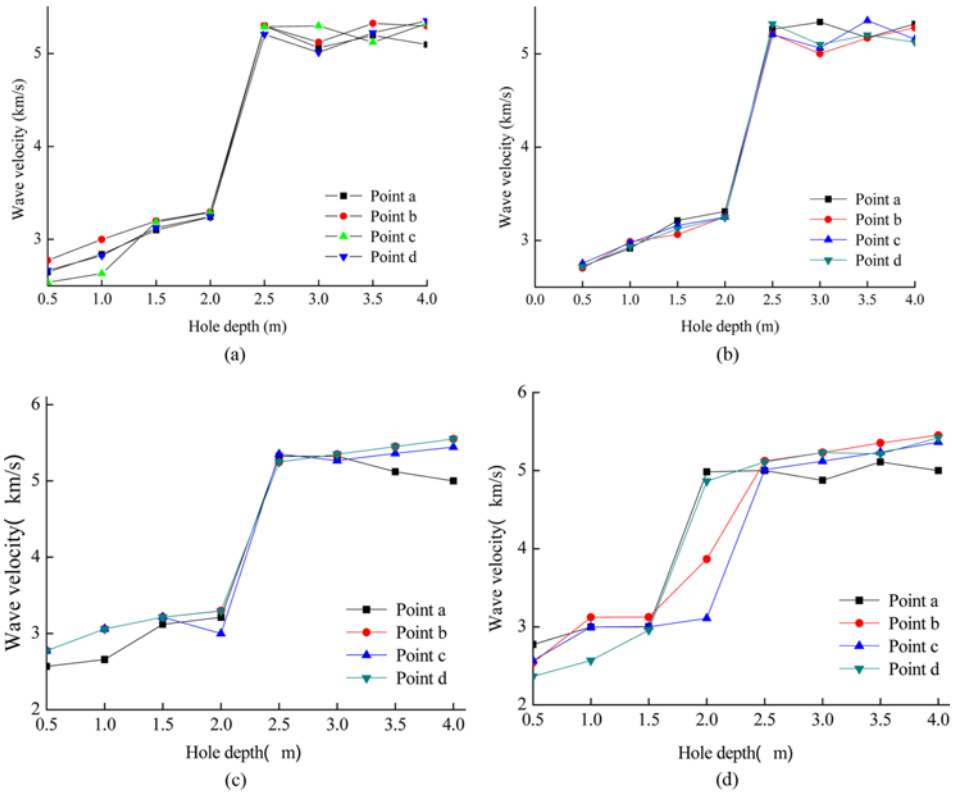

Fig. 12. Hole Depth–wave Velocity Curve of V: (a) YK184+825 Section, (b) YK191+690 Section, (c) ZK183+580 Section, (d) ZK183+550 Section

Table 8. Loose Circle Thickness

Level	Section	Point	v_{yl} (km/s)	L_v	v_{pl} (km/s)	Thickness D (m)
III	YK186+025	a	6.263	0.53	4.559	0.63
		b	6.318		4.600	0.67
		c	6.191		4.507	0.74
		d	6.439		4.687	0.75
	YK186+110	a	6.673		4.858	0.65
		b	5.478		3.988	0.55
		c	6.783		4.938	0.82
		d	6.673		4.858	0.73
	ZK185+831	a	6.241		4.544	0.62
		b	6.303		4.588	0.66
		c	6.124		4.458	0.74
		d	6.415		4.670	0.60
	ZK185+447	a	6.117		4.453	0.50
		b	6.779		4.935	0.65
		c	6.123		4.457	0.65
		d	6.230		4.535	0.63
IV	YK183+590	a	5.968	0.45	4.003	0.81
		b	6.085		4.082	1.02
		c	5.942		3.986	1.19
		d	6.014		4.034	1.10
	YK183+610	a	5.707		3.828	1.03
		b	5.509		3.696	1.12
		c	6.138		4.118	1.21
		d	5.811		3.898	1.51
	ZK183+647	a	6.280		4.213	1.19
		b	5.979		4.011	1.20
		c	6.085		4.082	1.10
		d	6.070		4.072	1.09
	ZK184+665	a	6.280		4.213	1.19
		b	6.059		4.064	1.00
		c	5.814		3.900	1.37
		d	5.643		3.786	1.22
V	YK184+825	a	5.160	0.39	3.220	1.93
		b	5.260		3.282	1.93
		c	5.300		3.276	1.94
		d	5.190		3.239	1.97
	YK191+690	a	5.275		3.292	1.9
		b	5.165		3.223	1.92
		c	5.195		3.242	1.95
		d	5.186		3.236	1.96
	ZK183+580	a	5.098		3.184	1.99
		b	5.401		3.373	2.07
		c	5.427		3.389	2.10
		d	5.486		3.3426	2.03
	ZK183+550	a	4.995		3.119	1.53
		b	5.290		3.303	1.62
		c	5.184		3.237	2.03
		d	5.168		3.228	1.57

0.81–1.79 and 1.53–2.24 m, respectively. Thus, the theoretical calculation formula that we deduced is reasonable and can be applied to this tunnel engineering.

Table 9. Comparison of Measured and Calculated Thicknesses of Loose Circle (m)

Location		Field test	H–B criterion	H–B considering intermediate principal stress
III	Arch	0.60–0.82	1.69	0.82
	Sidewall	0.50–0.67	1.34	0.69
IV	Arch	1.09–1.51	3.20	1.79
	Sidewall	0.81–1.20	2.98	1.37
V	Arch	1.57–2.10	3.95	2.24
	Sidewall	1.53–2.07	3.74	2.10

4. Conclusions

Determining the loose circle radius of surrounding rock by theoretical formula is always the hotspot and difficult points in engineering and academic research. A formula for the loose circle radius of surrounding rocks is deduced by considering intermediate principal stress and the Lode parameter on the basis of the H–B criterion. The distribution of loose circles in three-lane hard rock tunnels is studied by regarding Shimen Tunnel engineering as an example. The main conclusions are as follows.

1. From the current research, intermediate principal stress considerably influences the surrounding rock loose circle. Therefore, the H–B criterion is modified by considering intermediate principal stress, and the loose circle thickness of the surrounding rock is deduced on the basis of the modified formula.
2. Put forward a new criterion to determine the loose circle, the integrity coefficients of broken rock (R_v) and loose circle (L_v) are introduced. R_v is the square of ratios between the longitudinal wave velocity (v_{pr}) of broken rock and the longitudinal wave velocity (v_{wr}) of intact rock. L_v is the square of the ratios between the longitudinal wave velocity (v_{pl}) in the position of the broken rock loose circle and the longitudinal wave velocity (v_{yl}) of the initial rock mass. The loose zone is essentially a relaxation fracture zone. Therefore, R_v can be considered equal to L_v during the deduction process. By combining these formulas, v_{pl} is obtained. The position where the longitudinal wave velocity value in the hole depth–wave velocity curve is equal to v_{pl} is the boundary of the loose circle.
3. The deduced formula is applied to the Shimen Tunnel. The results of the field acoustic wave test show consistency between the results of the theoretical calculations and field measurements. The theoretical analysis and field test demonstrate that the specific value ranges of the loose circle are 0.50–0.82, 0.81–1.79 and 1.53–2.24 m in levels III, IV and V surrounding rocks, respectively. Loose circles are evenly distributed in the tunnel cross sections, and the arch value is generally larger than the waist value.
4. From the theoretical analysis, the Lode parameter has a direct relationship with the intermediate principal stress. Intermediate principal stress can be reflected in the formula by considering this parameter. With an increase in Lode

parameter (Intermediate principal stress enlarges.), loose circle radius decreases. At this time, Lode parameter and loose circle radius exist a negative linear correlation and a negative value appears (No loose circle exists.). Therefore, with the increase of intermediate principal stress, the rock strength increases and the rock-crushing disturbance becomes increasingly difficult to control. Therefore, the loose circle is getting smaller and even the loose circle thickness is zero.

Acknowledgments

This research was financially supported by the National Natural Science Foundation of China Grant [No. 51679199]; the Natural Science Basic Research by Shaanxi Province Grant [2017JM5136]; the Key Laboratory Program by Shaanxi Provincial Science Grant [2014SZS15-Z01]; the Housing and Urban-Rural Construction Foundation by the Housing and Urban-Rural Department of Shaanxi Province Grant [2017-K55]; the Scientific Research Program for Technology of Highway Construction and Maintenance Technology of National Transportation Industry Key Laboratory Grant [KLTLR-Y14-15] and Technology Innovation and the Research Program sponsored by Xi'an Technological University President Fund Grant [XAGDXJJ16003].

References

Bezalel, H. and John, W. (2010). "The effect of the intermediate principal stress on fault formation and fault angle in siltstone." *Journal of Structural Geology*, Vol. 32, No. 11, pp. 1701-1711, DOI: 10.1016/j.jsg.2009.08.017.

Cai, M. (2008). "Influence of intermediate principal stress on rock fracturing and strength near excavation boundaries—insight from numerical modeling." *International Journal of Rock Mechanics and Mining Sciences*, Vol. 45, No. 5, pp. 763-772, DOI: 10.1016/j.ijrmms.2007.07.026.

Cao, P., Chen, C., Zhang, K., Pu, C. Z., and Liu, T. (2014). "Measurement and analysis of deep roadway surrounding rock loose zone in Jinchuan mine." *Journal of Central South University (Science and Technology)*, Vol. 45, No. 8, pp. 2839-2844.

Chen, Q. N., Huang, X. C., and Xie, X. Y. (2015). "Deduction and improvement of surrounding rock loose circle radius based on Hoek-Brown criterion." *Chinese Journal of Applied Mechanics*, Vol. 32 No. 2, pp. 304-310+357-358.

Dai, J., Yang, F., Wu, Y., and Zou, Q. Q. (2014). "Application of RSMSY5(N) acoustic-waves-monitor in releasing zone measuring and test." *Coal Technology*, Vol. 33, No. 12, pp. 76-78, DOI: 10.13301/j.cnki.ct.2014.12.027.

Dong, F. T., Song, H. W., Guo, Z. H., Lu, S. M., and Liang, S. J. (1994). "Support theory of surrounding rock loose circle." *Journal of China Coal Society*, Vol. 19, No. 1, pp. 21-31.

Frederic, L. and Geraldine, F. (2007). "Damage evaluation with p-wave velocity measurements during uniaxial compression tests on argillaceous rocks." *International Journal of Geomechanics*., Vol. 7, No. 6, pp. 431-436, DOI: 10.1061/(asce)1532-3641(2007)7:6(431).

Hua, J. (2017). "Three-dimensional failure criteria for rocks based on the hoek–brown criterion and a general lode dependence." *International Journal of Geomechanics.*, Vol. 17, No. 8, pp. 04017023, 1-12, DOI: 10.1061/(asce)gm.1943-5622.0000900.

Huang, F., Zhu, H. H., Li, Q. S., and Li, E. P. (2016). "Field detection and theoretic analysis of loose circle of rock mass surrounding tunnel." *Rock and Soil Mechanics*, Vol. 37, No. S1, pp. 145-150, DOI: 10.16285/j.rsm.2016.S1.019.

Li, N., Duan, X. Q., Chen, F. F., and Yuan, J. G. (2006). "A back analysis method for elastoplastic displacement of broken rock zone around tunnel." *Chinese Journal of Rock Mechanics and Engineering*, Vol. 5, No. 7, pp. 12-16.

Li, W. L., Wang, L., and Chang, J. C. (2011). "Calculation and site measurement of surrounding rock released circle base on Hoek-Brown criterion." *Coal Engineering*, No. 2, pp. 97-99.

Li, Z. L., Wu, R. X., and Li, L. J. (2011). "Method for defining the loose zone of tunnel surrounding rock based on damage theory." *Chinese Journal of Underground Space and Engineering*, Vol. 7, No. 6, pp. 1060-1064.

Melkoumian, N., Priest, S., and Hunt, S. (2009). "Further development of the three-dimensional Hoek-Brown yield criterion." *Rock Mechanics and Rock Engineering*, Vol. 42, No. 6, pp. 835-847, DOI: 10.1007/s00603-008-0022-0.

Ren, Q. W. and Zhang, H. C. (2001). "A modification of fenner formula." *Journal of Hohai University*, Vol. 9, No. 6, pp. 109-111.

Rennie, K. (2014). "New artificial neural networks for true triaxial stress state analysis and demonstration of intermediate principal stress effects on intact rock strength." *Journal of Rock Mechanics and Geotechnical Engineering*, No. 6, pp. 338-347, DOI: 10.1016/j.jrmge.2014.04.008.

Serrano, A., Olalla, C., and Reig, I. (2011). "Convergence of circular tunnels in elastoplastic rock masses with non-linear failure criteria and non-associated flow laws." *Rock Mechanics and Mining Sciences*, No. 43, pp. 878-887, DOI: 10.1016/j.ijrmms.2011.06.008.

Shen, Y. J., Xu, G. L., Zhang, L., and Zhu, K. J. (2010). "Research on characteristics of rock deformation caused by excavation disturbance based on Hoek-Brown criterion." *Chinese Journal of Rock Mechanics and Engineering*, Vol. 29, No. 7, pp. 1355-1362.

Singh, B., Goel, R. K., Mehrotra, V. K., Garg, S. K., and Allu, M. R. (1998). "Effect of intermediate principal stress on strength of anisotropic rock mass." *Tunneling and Under-ground Space Technology*, Vol. 13, No. 1, pp. 71-79, DOI: 10.1016/s0886-7798(98)00023-6.

Sriapai, T., Walsri, C., and Fuenkajorn, K. (2013). "True-triaxial compressive strength of Maha Sarakham salt." *International Journal of Rock Mechanics and Mining Sciences*, No. 61, pp. 256-265, DOI: 10.1016/j.ijrmms.2013.03.010.

Sun, X. K., Chang, Q.L., Shi, X. Y., and Li, X. Y. (2016). "Thickness measurement and distribution law of loose rings of surrounding rock in large cross section semicircle arch seam gateway." *Coal Science and Technology*, Vol. 44, No. 11, pp. 1-6, DOI: 10.13199/j.cnki.cst.2016.11.001.

Wang, C. H., Guo, Q. L., and Jia, L. (2011). "Theoretical analysis of high stress criterion based on the Hoek-Brown criterion." *Rock and Soil Mechanics*, Vol. 32, No. 11, pp. 3325-3332, DOI: 10.16285/j.rsm.2011.11.015.

Wang, Y. C., Jing, H. W., Su, H. J., and Xie, J. Y. (2017). "Effect of a fault fracture zone on the stability of tunnel-surrounding rock." *International Journal of Geomechanics*., Vol. 16, No. 6, pp. 04016135,1-20, DOI: 10.1061/(asce)gm.1943-5622.0000837.

Wu, T., Dai, J., Du, M. L., Wu, Y., and Gao, Y. Z. (2015). "Surrounding rock loosing circle test based on acoustic test technology." *Safety in Coal Mines*, Vol. 46, No. 1, pp. 169-172, DOI: 10.13347/j.cnki.mkaq.2015.01.049.

Xu, D. J. and Geng, N. G. (1985). "Variation law of rock strength with intermediate principal stress." *Acta Mechanica Solida Sinica*," No. 1, pp. 72-80, DOI: 10.19636/j.cnki.cjsm42-1250/o3.1985.01.007.

Yu, D. M., Fan, Y. F., Duan, J. X., and Luo, X. W. (2013). "Elastoplastic unified solutions to deep-buried circular tunnels considering intermediate principal stress." *Journal of Shanghai Jiao Tong University*, Vol. 47, No. 9, pp. 1447-1453.

Yu, D. M., Yao, H. L., Lu, Z., and Luo, X. W. (2012). "Elastoplastic solutions to deep-buried circular tunnels in transversely isotropic rock masses considering intermediate principal stress." *Chinese Journal of Geotechnical Engineering*, Vol. 34, No. 10, pp. 1850-1857.

Zhang, H. L., Liu, T., Guo, S. M., Sun, J., and Wang, C. C. (2014). "Loose circle distribution survey of roadway surrounding rock of isolation pillar." *Metal Mine*, No. 7, pp. 151-155.

Zhang, X. Y., Li, Z., and Zhu, S. A. (2016). "Support technique of deep soft rock roadway based on loose circle test of surrounding rock." *Safety in Coal Mines*, Vol. 47, No. 5, pp. 94-100, DOI: 10.13347/j.cnki.mkaq.2016.05.024.

Zhou, X. S. and Song, H. W. (1994). "Theory research situation of foreign surrounding rock loose circle support theory." *Well Drilling Technology*, No. Z1, pp. 67-71.

Zou, J. F. and Su, Y. (2016). "Theoretical solutions of a circular tunnel with the influence of the Out-of-Plane stress based on the generalized Hoek–Brown failure criterion." *International Journal of Geomechanics*, Vol. 16, No. 3, pp. 1-10, DOI: 10.1061/(ASCE)GM.1943-5622.0000547.